Synchronized Oscillations in the Inferior Olive Are Controlled by the Hyperpolarization-Activated Cation Current I_h

THIERRY BAL[1] AND DAVID A. McCORMICK[2]
[1]*Institut Alfred Fessard, Centre National de la Recherche Scientifique, Gif sur Yvette, Cedex 91198, France; and*
[2]*Section of Neurobiology, Yale University School of Medicine, New Haven, Connecticut 06473*

Bal, Thierry and David A. McCormick. Synchronized oscillations in the inferior olive are controlled by the hyperpolarization-activated cation current I_h. *J. Neurophysiol.* 77: 3145–3156, 1997. The participation of a hyperpolarization-activated cationic current in the generation of oscillations in single inferior olive neurons and in the generation of ensemble oscillations in the inferior olive nucleus (IO) of the guinea pig and ferret was investigated in slices maintained in vitro. Intracellular recordings in guinea pig or ferret IO neurons revealed that these cells could generate sustained endogenous oscillations (4–10 Hz) at hyperpolarized membrane potentials (−60 to −67 mV) after the intracellular injection of a brief hyperpolarizing current pulse. These oscillations appeared as the rhythmic generation of a low-threshold Ca^{2+} spike that typically initiated one or two fast Na^+-dependent action potentials. Between low-threshold Ca^{2+} spikes was an afterhyperpolarization that formed a ''pacemaker'' potential. Local application of apamin resulted in a large reduction in the amplitude of the afterhyperpolarization, indicating that a Ca^{2+}-activated K^+ current makes a strong contribution to its generation. However, even in the presence of apamin, hyperpolarization of IO neurons results in a ''depolarizing sag'' of the membrane potential that was blocked by local application of Cs^+ or partial replacement of extracellular Na^+ with choline$^+$ or *N*-methyl-D-glucamine$^+$, suggesting that I_h also contributes to the generation of the afterhyperpolarization. Extracellular application of low concentrations of cesium resulted in hyperpolarization of the membrane potential of IO neurons and spontaneous 5- to 6-Hz oscillations in single, as well as networks, of IO neurons. Application of larger concentrations of cesium reduced the frequency of oscillation to 2–3 Hz or blocked the oscillation entirely. On the basis of these results, we propose that I_h contributes to single and ensemble oscillations in the IO in two ways: *1*) I_h contributes to the determination of the resting membrane potential such that reduction of I_h results in hyperpolarization of the membrane potential and an increased propensity of oscillation through removal of inactivation of the low-threshold Ca^{2+} current; and *2*) I_h contributes to the generation of the afterhyperpolarization and the pacemaker potential between low-threshold Ca^{2+} spikes.

INTRODUCTION

Inferior olivary neurons densely innervate and monosynaptically excite cerebellar Purkinje cells through characteristic axonal terminations known as climbing fibers, and thus form a major afferent pathway to the cerebellar cortex (Eccles et al. 1966). Inferior olivary neurons fire at a frequency of 1–12 Hz and can exhibit spontaneous oscillatory activity near 10 Hz (Armstrong et al. 1968). Likewise, the resulting complex spikes occurring in Purkinje cells are also rhythmic and display a maximum frequency of 10–12 Hz (Llinás and Sasaki 1989). Simultaneous recordings from several Purkinje cells have revealed that complex spikes can occur synchronously, suggesting that ensembles of inferior olive nucleus (IO) neurons have the ability to fire rhythmically in unison (Bell and Kawasaki 1972; Bower and Llinás 1983; Fukuda et al. 1987; Llinás and Volkind 1973; Sasaki and Llinás 1985; Yamamoto et al. 1986). This synchronous oscillation has been proposed to be important in the determination of the timing and dynamic organization of motor sequences in motor coordination (Llinás 1988; Llinás and Welsh 1993; Vallbo and Wessberg 1993), a hypothesis that is supported by studies in which multiple recordings from Purkinje cells in the rat cerebellum were used (Llinás and Sasaki 1989; Welsh et al. 1995).

Intracellular recordings from inferior olivary neurons maintained as a slice in vitro revealed that these cells have the intrinsic properties necessary not only to endogenously oscillate but also to influence one another through electrotonic gap junctions (Llinás and Yarom 1981a,b) and thereby generate pools of synchronously oscillating neurons (Benardo and Foster 1986; Llinás and Yarom 1986). These ensemble oscillations can appear as either subthreshold sine-wave-shaped oscillations of the membrane potential or as the rhythmic generation of low-threshold Ca^{2+} spikes, and they can occur either spontaneously or in response to the application of the alkaloid harmaline (Benardo and Foster 1986; Llinás and Yarom 1986). Interestingly, harmaline, when administered in vivo, results in a 10-Hz tremor, presumably through the induction of oscillations in the inferior olive (de Montigny and Lamarre 1973; Llinás and Volkind 1973).

Pioneering in vitro studies by Llinás and Yarom (1981a,b) have described many of the ionic conductances that underlie the endogenous oscillatory properties of single IO neurons, as well as these neurons' ability to generate ensemble oscillations in the 4- to 10-Hz range through electrotonic coupling (Llinás and Yarom 1981a, 1986; Llinás et al. 1974). Three main conductances, in addition to those involved in action potential generation, have been proposed to account for the oscillatory properties of IO neurons: a dendritic high-threshold Ca^{2+} conductance, a somatic low-threshold Ca^{2+} conductance, and a Ca^{2+}-activated K^+ conductance (Llinás and Yarom 1981a,b). The interaction of the high-threshold Ca^{2+} current and the prominent Ca^{2+}-activated K^+ current was proposed to account for the generation of low-frequency firing (up to 6 Hz), whereas higher-frequency (up to 10 Hz) firing was proposed to occur at more hyperpolarized membrane potentials with less involvement of the high-threshold Ca^{2+} current.

0022-3077/97 $5.00

In similarity with inferior olivary neurons, thalamocortical relay neurons also possess the endogenous ability to generate rhythmic oscillations (Jahnsen and Llinás 1984a,b; McCormick and Pape 1990a; Soltesz et al. 1991). Detailed examination of the mechanisms of oscillation in single thalamic relay neurons has revealed a critical role for the hyperpolarization-activated cation current known as I_h (McCormick and Huguenard 1992; McCormick and Pape 1990a; Soltesz et al. 1991). Low-frequency (0.5–4 Hz) rhythmic burst firing can be generated in thalamocortical neurons through the interaction between the low-threshold Ca^{2+} current I_T and I_h. In this manner, the activation/inactivation of I_T results in the generation of low-threshold Ca^{2+} spikes and high-frequency bursts of Na^+-dependent action potentials and the activation/deactivation of I_h provides a ''pacemaker-potential'' that times the generation of these low-threshold Ca^{2+} spikes (McCormick and Huguenard 1992; McCormick and Pape 1990a). Interestingly, alterations in the amplitude or voltage dependence of activation/deactivation of I_h can have strong effects on both the ability of thalamocortical relay neurons to endogenously oscillate and the frequency of this oscillation (McCormick and Huguenard 1992; McCormick and Pape 1990a,b; McCormick and Williamson 1991). Partial reduction of I_h in thalamocortical relay neurons results in the enhancement of rhythmic oscillation, whereas complete block of I_h results in an abolition of endogenous oscillations (McCormick and Pape 1990a).

Hyperpolarization of inferior olivary neurons results in a strong ''depolarizing sag'' (Yarom and Llinás 1987) that is likely the result of activation of a hyperpolarization-activated cation current. This anomalous rectification in the hyperpolarizing range is blocked by extracellular application of harmaline and extracellular Cs^+ (Yarom and Llinás 1987). Together with previous results in thalamocortical relay neurons, these results suggest that I_h may also play an important role in the determination of the occurrence and frequency of oscillations in the inferior olive and that the reduction of this current may be the major mechanism by which harmaline induces rhythmic oscillations in this nucleus. In the present study, we demonstrate that I_h can potently modulate the presence and frequency of single and ensemble oscillations in the inferior olive.

METHODS

Male or female adult Hartley guinea pigs or ferrets, 2–9 mo old, were deeply anesthetized with pentobarbital sodium (30–40 mg/kg) and killed by decapitation. The brain was rapidly removed and the region of the brain stem containing the inferior olive was dissected free. Slices 400 μm thick were cut in the coronal plane with the use of a Vibratome (Ted Pella). A modification of the technique developed by Aghajanian and Rasmussen (1989) was used to increase tissue viability. During preparation of slices, the tissue was placed in the normal slice bathing solution (5°C), except that NaCl was replaced with sucrose while an osmolarity of 307 mosM was maintained. After preparation, slices were placed in an interface-style recording chamber (Fine Sciences Tools) and allowed ≥2 h to recover. The normal bathing medium contained (in mM) 126 NaCl, 2.5 KCl, 1.2 $MgSO_4$, 1.25 NaH_2PO_4, 2 $CaCl_2$, 26 $NaHCO_3$, and 10 dextrose, aerated with 95% O_2-5% CO_2 to a final pH of 7.4. For the first 20 min the inferior olivary slices were in the recording chamber, the bathing medium contained an equal mixture of the normal-NaCl and the sucrose-substituted solutions. After the 2 h of recovery, extracellular multiple-unit recordings were performed from multiple locations in each slice to determine the prevalence of spontaneous spiking activity. Recordings were performed with the slices between the temperatures of 34.5 and 35.5°C.

Cesium acetate was dissolved in the bathing medium (1–2 mM) or was applied with the pressure-pulse technique (10–20 mM in the micropipette), in which a brief pulse of pressure (10–100 ms, 200–350 kPa) to a broken micropipette (tip diameter 2–10 μm) was used to extrude volumes of 2–20 pl. Extracellular multiple-unit recordings were obtained with tungsten microelectrodes (Frederick Haer, Brunswick, ME), whereas intracellular recordings were obtained with glass microelectrodes formed on a Sutter Instruments (Novato, CA) P-80/PC micropipette puller, filled with 1.2 or 4 M potassium acetate, and beveled to a final resistance of 70–100 MΩ. Beveled electrodes were found to be necessary in our experiments to obtain recordings from IO neurons that retained the ability to generate intrinsic and prolonged oscillations. Electrical stimulation was performed with the use of bipolar tungsten electrodes similar to those used for extracellular recordings. Tips were electroplated with gold in a 2% $HAuCL_4$ solution with the use of a 1.5-V battery as a current generator. Stimulations (25–250 μA, duration 0.1 ms) were delivered as one to three shocks with an intershock interval of 10 ms. All data are presented as means ± SD.

RESULTS

Intracellular recordings were obtained from guinea pig (n = 48) and ferret (n = 17) inferior olivary neurons. In addition, simultaneous extracellular multiple-unit recordings were routinely performed to monitor neuronal population activity (e.g., see Fig. 1*A*). Recordings in both species revealed similar results and therefore were combined for analysis. Extracellular and intracellular recordings from IO neurons revealed that these cells were typically silent at rest (Figs. 1 and 2). In contrast, electrical stimulation of the slice near the IO resulted in a typical 6- to 10-Hz rhythmic bursting activity in both the extracellularly recorded multiple-unit activity and intracellularly recorded single neuron. These rhythmic oscillations could be either supra- or subthreshold for the generation of action potential activity. Simultaneous extracellular and intracellular recordings at neighboring sites revealed that these ensemble oscillations were synchronous for the cells recorded (Fig. 1*A*).

In cells at resting membrane potential, intracellular injection of a hyperpolarizing current pulse 0.1–1 s (typically 200 ms) in duration was followed by a rebound low-threshold Ca^{2+} spike (Yarom and Llinás 1987), which itself triggered between zero and two fast, Na^+-dependent action potentials (Figs. 1*B* and 2, *A* and *B*). On occasion, the offset of the hyperpolarizing current pulse was followed by a brief period of damped oscillation (e.g., Fig. 2*A*, −57 mV). Hyperpolarization of inferior olivary neurons to the voltage range of approximately −60 to −67 mV with intracellular injection of DC resulted in 4- to 8-Hz oscillations being triggered by the offset of the same hyperpolarizing current pulses (Figs. 1*B* and 2*A; n* = 18). The frequency of these oscillations decreased over time and the oscillations terminated after several seconds (up to 30 s and 170 oscillation cycles) and were not critically dependent on the generation of fast Na^+ spikes (Fig. 2*A*, ↙), although fast spikes were shown to facilitate the generation of the oscillation (see Fig. 9 below). Further hyperpolarization of inferior olive cells with DC to membrane potentials of −70 mV or more

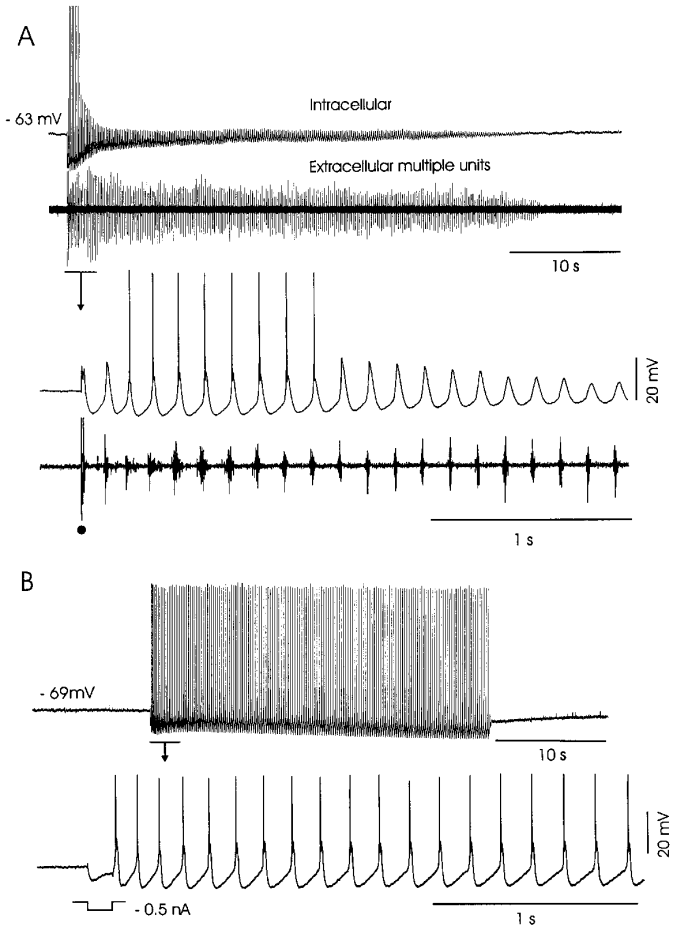

FIG. 1. Ensemble and single-cell oscillation in inferior olivary nucleus (IO). *A*: electrical stimulation of slice (●) outside border of IO induces synchronous oscillatory and rhythmic bursting activity in intracellular and extracellular multiple-unit recordings. First few s of oscillation are expanded for detail (↓). Note synchronization of activity of single intracellularly recorded neuron and multiple-unit activity. Intracellular and extracellular electrodes were spaced ~100 μm apart. *B*: in a different cell, injection of a brief hyperpolarizing pulse of current induces an intrinsic single-cell oscillation, the duration and frequency of which are similar to those of the ensemble oscillation shown in *A*. Cells in *A* and *B* were slightly hyperpolarized (5–10 mV) by a holding current. Action potentials in intracellular recordings are not shown at full height. Recording is from a guinea pig IO cell.

negative resulted in an abolition of rhythmic oscillations (Fig. 2*A*). Close examination of the rhythmic oscillations revealed that they were composed of low-threshold Ca^{2+} spikes that activated one or two fast Na^+-dependent action potentials and that were followed by pronounced afterhyperpolarizations (AHPs) (e.g., Fig. 2*A*, −70 mV), as described previously (Benardo and Foster 1986; Llinás and Yarom 1986) (see also below). These results indicate that IO cells, although typically not spontaneously oscillating at rest in vitro, possess all the necessary currents required to endogenously oscillate as individuals and as a network (Llinás and Yarom 1981a,b).

Evidence for the presence of I_h in inferior olivary cells

The enhancement of rhythmic oscillations in IO neurons with hyperpolarization suggests that currents activated by hyperpolarization, such as I_h, may contribute to this feature of IO electroresponsiveness. Indeed, examination of the response of IO neurons to the 200-ms hyperpolarizing current pulse revealed a substantial depolarizing sag (Fig. 2, *A* and *B*). The amplitude of this depolarizing sag decreased markedly on tonic hyperpolarization, as would be expected if this feature were generated by activation of I_h, because this current may be tonically activated at these membrane potentials (McCormick and Pape 1990a).

To more closely examine the properties of the depolarizing sag activated by hyperpolarization, a family of hyperpolarizing current pulses was injected into inferior olivary neurons (Fig. 2*C*). Progressive hyperpolarization of IO neurons resulted not only in progressively larger hyperpolarizations of the membrane potential, but also in activation of a progressively larger depolarizing sag, as well as progressively larger rebound low-threshold Ca^{2+} spikes (Fig. 2*C*).

Further evidence for the presence of I_h in IO neurons was obtained with local application of cesium chloride, which is known to specifically block this current in other neuronal systems (e.g., see McCormick and Pape 1990a). Local application of Cs^+ (several 10- to 20-pl drops of 10–20 mM CsCl in micropipette) to the region near the recorded IO neuron resulted in a reversible block of the depolarizing sag (Fig. 3) (Yarom and Llinás 1987). In addition, local application of Cs^+ hyperpolarized the cell from rest by 10–18 mV (14.8 ± 3.1 mV, mean ± SD; $n = 5$). This hyperpolarization could bring the membrane potential of the IO neuron below the threshold for activation of the low-threshold Ca^{2+} current and therefore prevent rebound low-threshold Ca^{2+} spikes (Fig. 3, *A* and *D*). Depolarization of the IO neurons back to the pre-Cs^+ membrane potential reinstated rhythmic rebound oscillations (Fig. 3). Comparison of the rebound oscillations in control versus Cs^+ revealed that extracellular application of Cs^+ resulted in a slowing of the frequency of oscillation (cf. Fig. 3, *B* and *C*). In addition, there was a slowing of the rate of rise of the offset of the AHP and on occasion an increase in the number of fast action potentials generated by the initial rebound low-threshold Ca^{2+} spike (from 1 to 2).

One complicating influence of the extracellular application of Cs^+ is that there is also an increase in the amplitude of membrane hyperpolarization in response to the intracellular injection of the current pulse (not shown). However, compensating for both the changes in membrane potential, with intracellular injection of DC, and the increase in electrotonic membrane response to the current pulse at steady state, by decreasing the amplitude of this current pulse, still resulted in a slowing of the frequency of rhythmic oscillation in IO neurons (mean increase of the 1st oscillation cycle duration: 28.1 ± 6.4%; $n = 6$) and a decrease in the rate of rise of the offset of the AHP (Fig. 4, *A*, *B*, and *D; n* = 6). These effects were reversible on washout of Cs^+ (Fig. 4*C*). Measurements of the duration of action potentials in the presence of Cs^+ revealed that they were not significantly changed in comparison with values obtained in normal medium (measures were made at the threshold of the 1st action potential generated in sequences of oscillations in 3 cells: 0.99 ± 0.06 ms, normal; 1.06 ± 0.05 ms, cesium).

The hyperpolarization of IO neurons in response to extracellular application of Cs^+ suggests that I_h may contribute to the resting membrane potential of these cells. If this is

the case, then depolarization of IO neurons should result in deactivation of I_h and removal of this depolarization would then lead to progressive (time-dependent) reactivation of I_h and thus give rise to an apparent AHP (e.g., McCormick and Pape 1990a). Such an I_h-dependent AHP would contribute to the large AHP that terminates rebound bursts in IO neurons and that has previously been demonstrated to be generated through the activation of a Ca^{2+}-activated K^+ current (Llinás and Yarom 1981a). Apamin, a potent blocker of some types of calcium-dependent potassium channels, applied locally

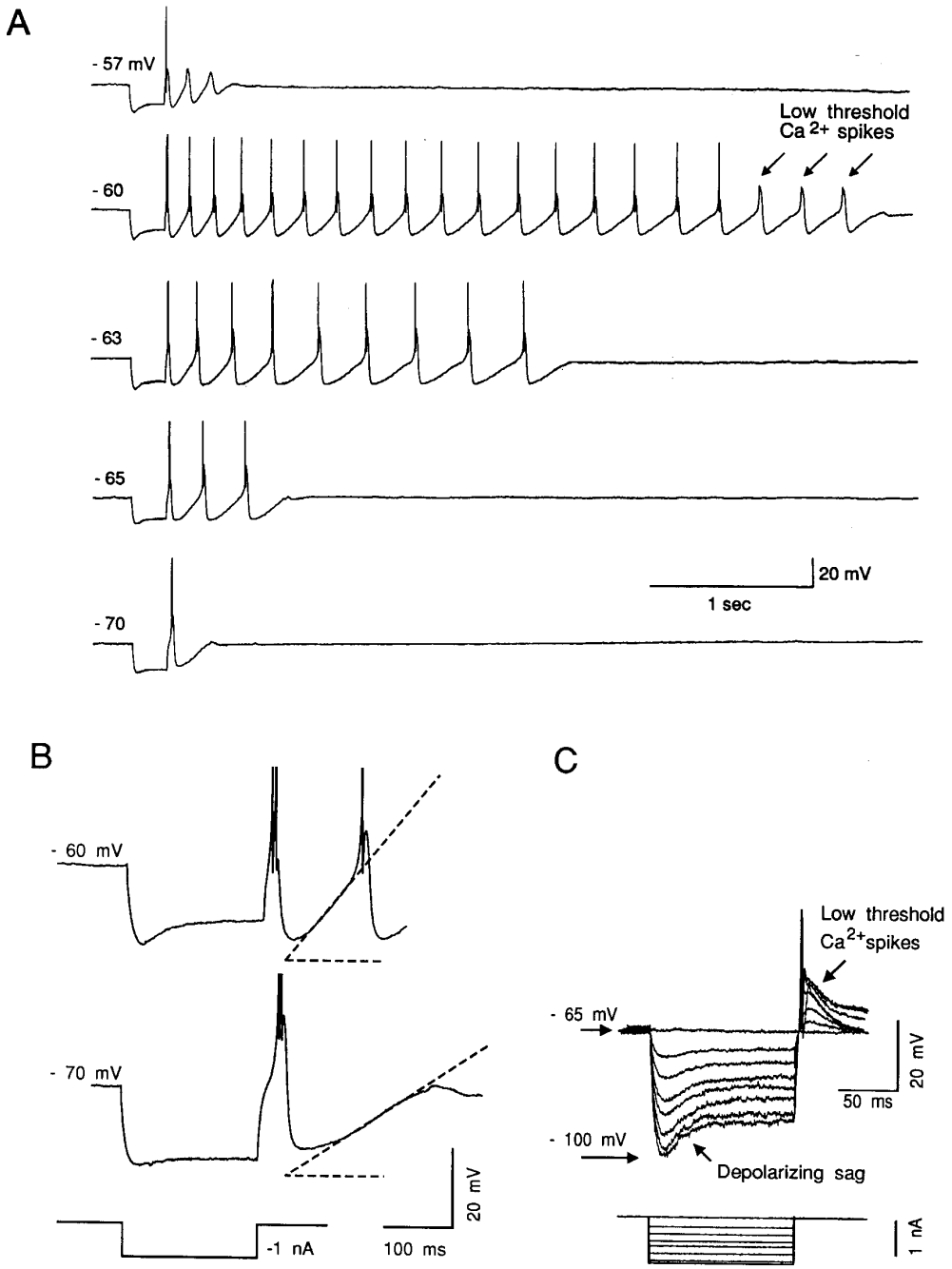

FIG. 2. Oscillatory properties of IO neurons and presence of hyperpolarization-activated rectification. *A*: intracellular injection of a hyperpolarizing current pulse at resting membrane potential of −57 mV resulted in a rhythmic oscillation consisting of 3 presumed low-threshold Ca^{2+} spikes interspersed by afterhyperpolarizations (AHPs). Intracellular injection of same current pulse after hyperpolarization of the IO neuron to −60 mV through intracellular injection of DC resulted in a prolonged (4-s) sequence of rhythmic oscillation, the frequency of which decreased over time. Last 3 low-threshold Ca^{2+} spikes failed to reach action potential threshold. Hyperpolarization of IO neuron to −63 and −65 mV decreased frequency and duration of oscillation. At −70 mV, oscillation was suppressed altogether and only 1 low-threshold Ca^{2+} spike and AHP were generated. *B*: comparing response of neuron to hyperpolarizing current pulse at −60 and −70 mV reveals decrease in ''depolarizing sag'' at −70 mV. *C*: intracellular injection of hyperpolarizing current pulses of progressively larger amplitude resulted in progressively larger hyperpolarizations, depolarizing sags, and rebound low-threshold Ca^{2+} spikes. Data obtained from ferret IO.

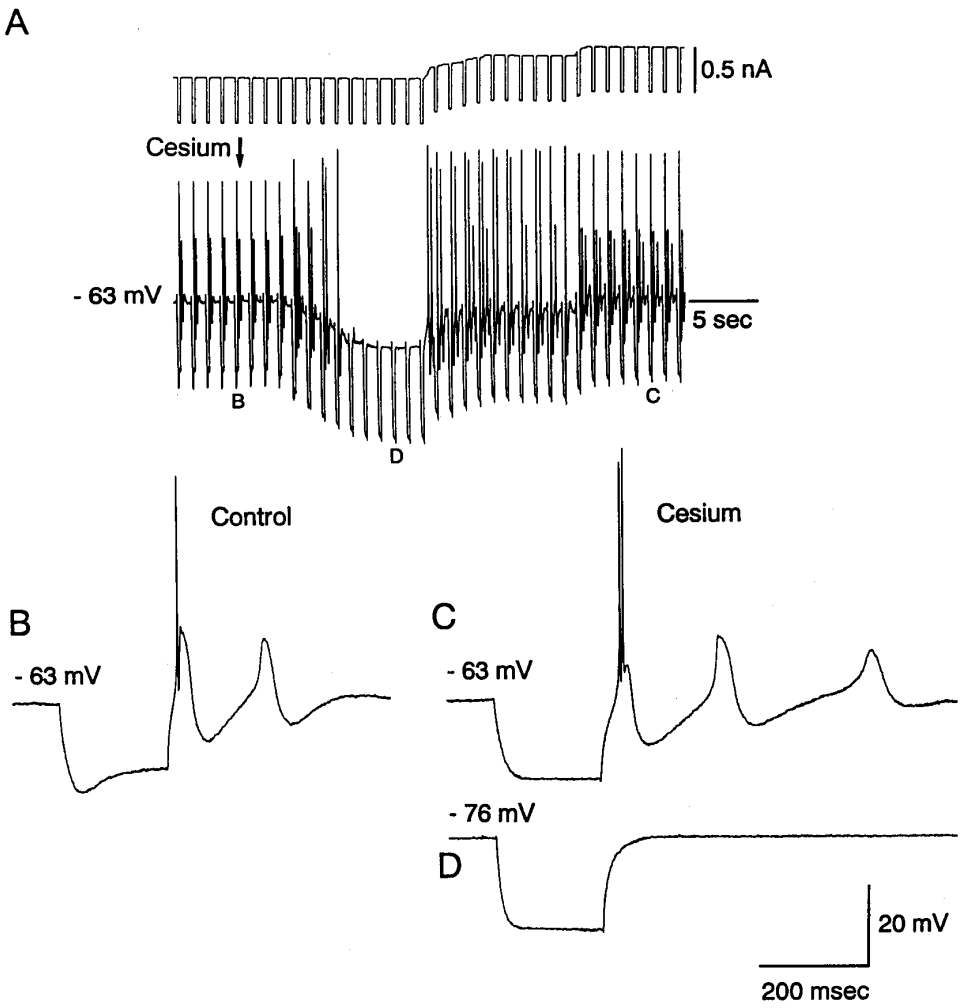

FIG. 3. Effects of extracellular application of Cs^+ on membrane potential and rhythmic oscillations in IO neurons. *A*: intracellular injection of hyperpolarizing current pulses at a rate of once every 2 s results in generation of a rhythmic sequence of 2 low-threshold Ca^{2+} spikes, interspersed with an AHP (*B*). Extracellular application of Cs^+ (20 mM in micropipette) resulted in hyperpolarization of membrane potential, abolition of depolarizing sag generated by hyperpolarizing current pulse (expanded in *D*), and abolition of rebound oscillations. Depolarization of cell back to −63 mV with intracellular injection of current (*A*, *top trace*) resulted in reinstatement of rhythmic oscillations, although depolarizing sag was completely blocked (expanded in *C*). Comparison of rhythmic oscillations generated on offset of current pulse before and after application of Cs^+ revealed a block of the depolarizing sag in the electrotonic response to the hyperpolarizing current pulse, an increase in amplitude of the rebound low-threshold Ca^{2+} spike, and a decrease in oscillation frequency. Data obtained from ferret IO.

(100 nM in micropipette), largely reduced the amplitude of the AHP, although a 2- to 4-mV AHP remained (Fig. 5*A; n* = 5); this residual AHP was reversibly blocked by local application of cesium with (Fig. 5*B; n* = 3) or without (not shown) compensation for the Cs^+-induced hyperpolarization of the membrane potential. The apparent AHP was still present even in the absence of calcium spikes or Na^+-dependent action potentials. These findings can be explained by taking into account the properties of I_h. The depolarization occurring during the generation of a low-threshold Ca^{2+} spike results in the deactivation of some portion of I_h. After the low-threshold Ca^{2+} spike, therefore, the membrane potential is allowed to achieve a more hyperpolarized level (owing to the deactivation of I_h) and generate an AHP. However, I_h once again activates and this slowly depolarizes the membrane potential, generating the rising phase of the AHP (see also McCormick and Pape 1990a).

If this hypothesis is true, the intracellular injection of a depolarizing current alone should result in the generation of an AHP. Indeed, removal of a prolonged depolarization of IO neurons was followed by the generation of an AHP, even if the prior depolarization was allowed to come to steady state and several seconds had passed since the generation of any low-threshold Ca^{2+} spikes (Fig. 6*A; n* = 10). Local application of Cs^+ resulted in an abolition of this AHP (Fig. 6*B*), an effect that was reversible (Fig. 6*C; n* = 4). Examination of this Cs^+-sensitive AHP revealed it to be ~100–400 ms in duration and 2–6 mV in amplitude (mean = 4.6 ± 1.2 mV; *n* = 4; Figs. 5 and 6). The depolarization-activated AHP remained unaltered after extracellular application of apamin (*n* = 2; Fig. 6*D*). The amplitude of this AHP was also dependent on the duration of the preceding depolarization (Fig. 6*D; n* = 2) and on its amplitude (not shown), as expected if I_h were involved in the generation of this AHP.

Contribution of I_h to rhythmic firing

Previous investigations in thalamocortical neurons revealed that extracellular application of Cs^+ could induce rhythmic oscillations in nonoscillating neurons through reduction of I_h (McCormick and Pape 1990a). The possibility that reduction of hyperpolarization-activated cation currents may also induce rhythmic oscillations in IO neurons was examined. In the example shown in Fig. 7, ensemble oscillations in the inferior olive were not present, as revealed with extracellular and intracellular recordings (Fig. 7*A*), although hyperpolarization of individual IO neurons could result in these cells generating sustained periods of rhythmic oscillation (Fig. 7*A*). Extracellular application of cesium chloride to the inferior olive, either locally via ejection from a micro-

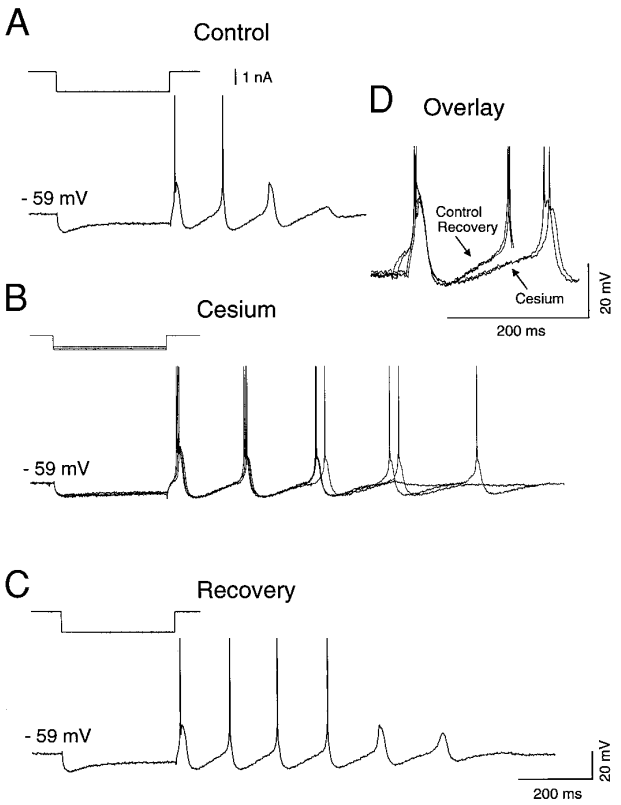

FIG. 4. Effect of cesium on oscillation frequency. *A*: intracellular injection of a hyperpolarizing current pulse results in a rebound rhythmic oscillation. Local application of Cs^+ (20 mM in micropipette) results in suppression of depolarizing sag and slowing by 30% of frequency of oscillation (*B*, *bottom*, overlay of 3 traces), an effect that is reversible (*C*). *D*: overlaying 1st cycle of oscillation for control, cesium, and recovery conditions reveals decrease of slope of pacemaker potential that results from cesium application. Intensity of holding current and of hyperpolarizing current pulses was adjusted to keep amount of hyperpolarization preceding calcium spike and membrane potential of cell the same before and after application of Cs^+. Data obtained from guinea pig IO.

pipette placed near (<50 μm) the recorded cell (5–20 mM in micropipette) or in the bath (1–2 mM), resulted in robust rhythmic activity in multiple IO neurons recorded extracellularly (Fig. 7, *B* and *C*). Cells recorded intracellularly in the vicinity of the multiple-unit electrode (at ~20 and 100 μm for *cells 2* and *3*, respectively) demonstrated membrane potentials that were more negative than in the absence of Cs^+, presumably resulting from the Cs^+-induced hyperpolarization of these cells (e.g., Fig. 3*A*). In the presence of Cs^+, intracellularly recorded IO neurons were found to oscillate at the same frequency as the ensemble oscillation (e.g., Fig. 7*C*, *cell 3*).

If the low-threshold Ca^{2+} spikes failed to occur during the Cs^+-induced ensemble oscillation (Fig. 7*C*), or were prevented through membrane depolarization or hyperpolarization (not shown), then rhythmic oscillations of the membrane were seen during these ensemble oscillations. These rhythmic oscillations were only seen when the extracellular multiple-unit recordings revealed rhythmic oscillations in the population of IO cells, and therefore presumably result from the electrotonically coupled activity of neighboring IO neurons, as reported previously (Benardo and Foster 1986; Llinás and Yarom 1986).

During the bath application of Cs^+, the frequency of oscillation generated by the inferior olive progressively decreased from 5–7 Hz to ~3 Hz (n = 4), presumably representing the slowly rising concentration of extracellular Cs^+ (Fig. 7*D*). These results indicate that extracellular application of cesium can both induce ensemble oscillations in inferior olive neurons and determine the frequency of oscillation. Because extracellular application of Cs^+ is known to block I_h in many cell types (Denyer and Brown 1990; DiFrancesco 1985; Halliwell and Adams 1982; Mayer and Westbrook 1983; McCormick and Pape 1990a; Spain et al. 1987; Tabata and Ishida 1996), these results suggest that this ionic current may play an important role in the determination of rhythmic oscillation in the inferior olive.

In other neuronal systems, hyperpolarization-activated cation currents have been demonstrated to be carried by both Na^+ and K^+ ions (Mayer and Westbrook 1983; McCormick and Pape 1990a; Tabata and Ishida 1996). The depolarizing sag in IO neurons is present even at membrane potentials positive to the presumed equilibrium potential for K^+ (approximately −100 mV), indicating that this feature is not mediated by the activation of a pure K^+ current. Indeed, substitution of choline

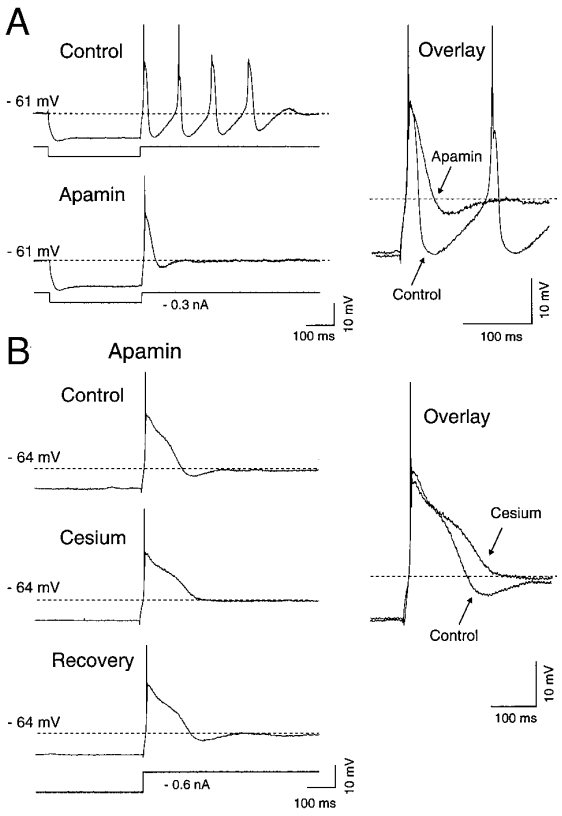

FIG. 5. Cesium- and apamin-sensitive AHPs are generated after a rebound burst. *A*: application of apamin (100 nM in micropipette) reduces amplitude of AHP, lengthens duration of low-threshold calcium spike, and suppresses rhythmic oscillations. *B*: extracellular application of cesium (20 mM in micropipette) on a different cell, in presence of apamin, reversibly blocks residual apamin-insensitive AHP and lengthens duration of low-threshold calcium spike. Large low-threshold calcium spikes in *B* were induced at offset of a 1-s hyperpolarizing current pulse. Intensity of holding current (in the −0.4-nA range) and of hyperpolarizing current pulses were adjusted to keep amount of hyperpolarization preceding calcium spike and membrane potential of cell constant. Data obtained from guinea pig IO.

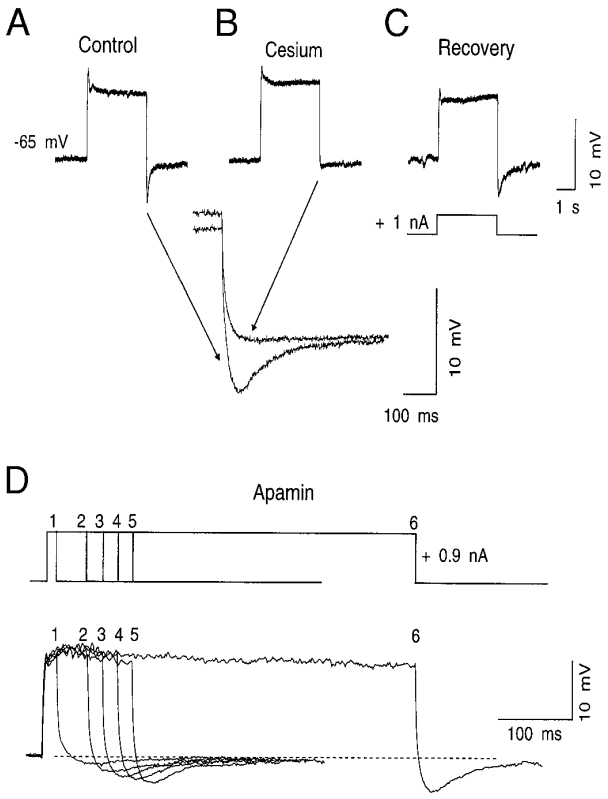

FIG. 6. Cesium blocks an AHP following a depolarizing current pulse. *A*: intracellular injection of a prolonged depolarizing current pulse is followed by generation of an AHP. *B*: local application of Cs^+ (20 mM in micropipette) resulted in a complete suppression of this AHP, an effect that was reversible (*C*). Arrows: expansion of AHP before and after local application of Cs^+. *D*: increasing duration of depolarizing current pulse results in a progressively larger AHP, presumably owing to progressive deactivation of I_h by the depolarization. Data obtained from ferret IO.

chloride for NaCl and choline bicarbonate for sodium bicarbonate in equimolar concentration in the bathing medium ($n = 3$) or of *N*-methyl-D-glucamine chloride (NMDG) for NaCl ($n = 3$), resulted in reduction of the depolarizing sag (Fig. 8, *F* and *G*) and in hyperpolarization of the cells by 10–24 mV (mean = 14.7 ± 5.3 mV; Fig. 8; $n = 6$). As the extracellular concentration of Na^+ was reduced and the membrane potential of IO neurons became more negative, rhythmic ''sine-wave'' oscillations appeared indicating that the IO was generating an ensemble oscillation (Fig. 8, *C* and *D; n* = 6). These oscillations could trigger low-threshold Ca^{2+} spikes, which were then in phase with the sine-wave oscillation (Fig. 8, *C* and *D*). As the extracellular concentration of Na^+ continued to decline, IO neurons hyperpolarized further and the ensemble oscillation ceased (Fig. 8*E*). These results are remarkably similar to those obtained with extracellular application of Cs^+ (see above) and suggest that at these membrane potentials the depolarizing sag is largely mediated by the inward movement of Na^+ ions.

Contribution of an apamin-sensitive K^+ current and Na^+ action potentials to the AHP

The presence of a large AHP following each low-threshold Ca^{2+} spike after blockade of I_h with extracellular Cs^+ (Figs. 3 and 4) indicates that additional ionic currents are involved in the generation of this electrophysiological feature. Indeed, block of fast Na^+ spikes activated by the low-threshold Ca^{2+} current with the local application of tetrodotoxin (TTX) (10 μM in micropipette) reduced the amplitude of the AHP (Fig. 9, *B* and *D*). Similarly, low-threshold Ca^{2+} spikes that did not generate fast action potentials were followed by an AHP that was smaller in amplitude than those that generate action potentials (not shown; $n = 4$). Interestingly, the application of TTX not only reduced the amplitude of the AHP, but also reduced the overall duration of the oscillation induced by the hyperpolarizing current pulse (Fig. 9*B*). Extracellular application of apamin (100 nM in micropipette) blocked the residual AHP remaining in the presence of Cs^+ and TTX (Fig. 9, *C* and *D*). In addition, local application of apamin also completely blocked the rhyth-

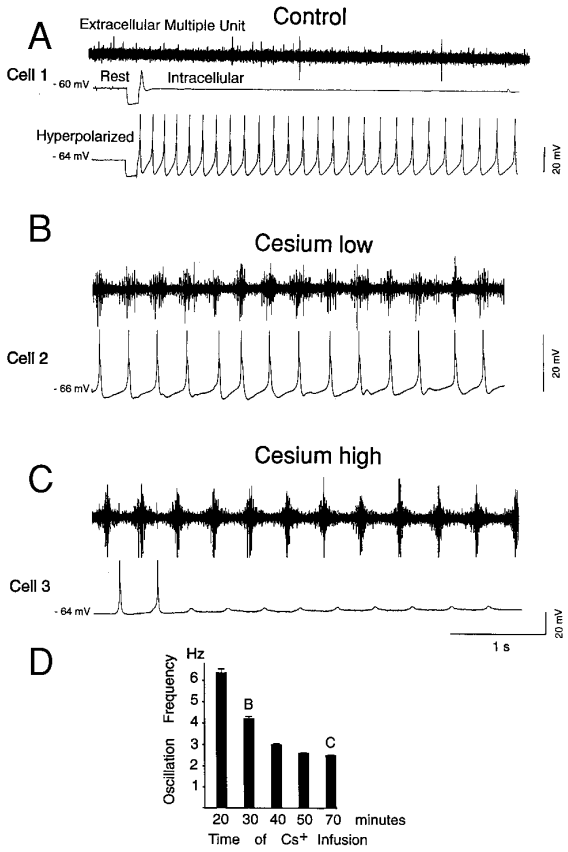

FIG. 7. Cesium induces synchronized ensemble oscillations in IO. *A*: extracellular recording from IO reveals absence of synchronized activity. Intracellular injection of a hyperpolarizing current pulse at resting potential typically did not result in rebound oscillations (*cell 1*), although these oscillations were evoked after hyperpolarization to −64 mV. Note that synchronized oscillations in extracellular multiple-unit recording were also absent during evoked generation of oscillations in a single cell. *B*: several minutes after addition of 2 mM Cs^+ to bathing medium, synchronized oscillations were prevalent in both an intracellularly recorded neuron (*cell 2*) and the extracellular multiple-unit recording. *C*: these oscillations continued, appeared to be even more synchronized, and slowed down in frequency when Cs^+ reached steady 2 mM concentration in bathing medium (1 h of infusion). Intracellular recordings revealed rhythmic generation of low-threshold Ca^{2+} spikes and subthreshold oscillations of membrane potential (*cell 3*). Phase of oscillation recorded in extracellular recordings and *cells 2* and *3* differed. This may have resulted from the fact that *cell 3* was recorded at an increased distance from the extracellular recording electrode in comparison with *cell 2*. *D*: plot of frequency of oscillation vs. time after switch to 2 mM Cs^+ in bathing medium. Recordings were performed in an interface-style recording chamber where change of ion concentrations does not reach steady state for ~30–40 min. Data obtained from ferret IO.

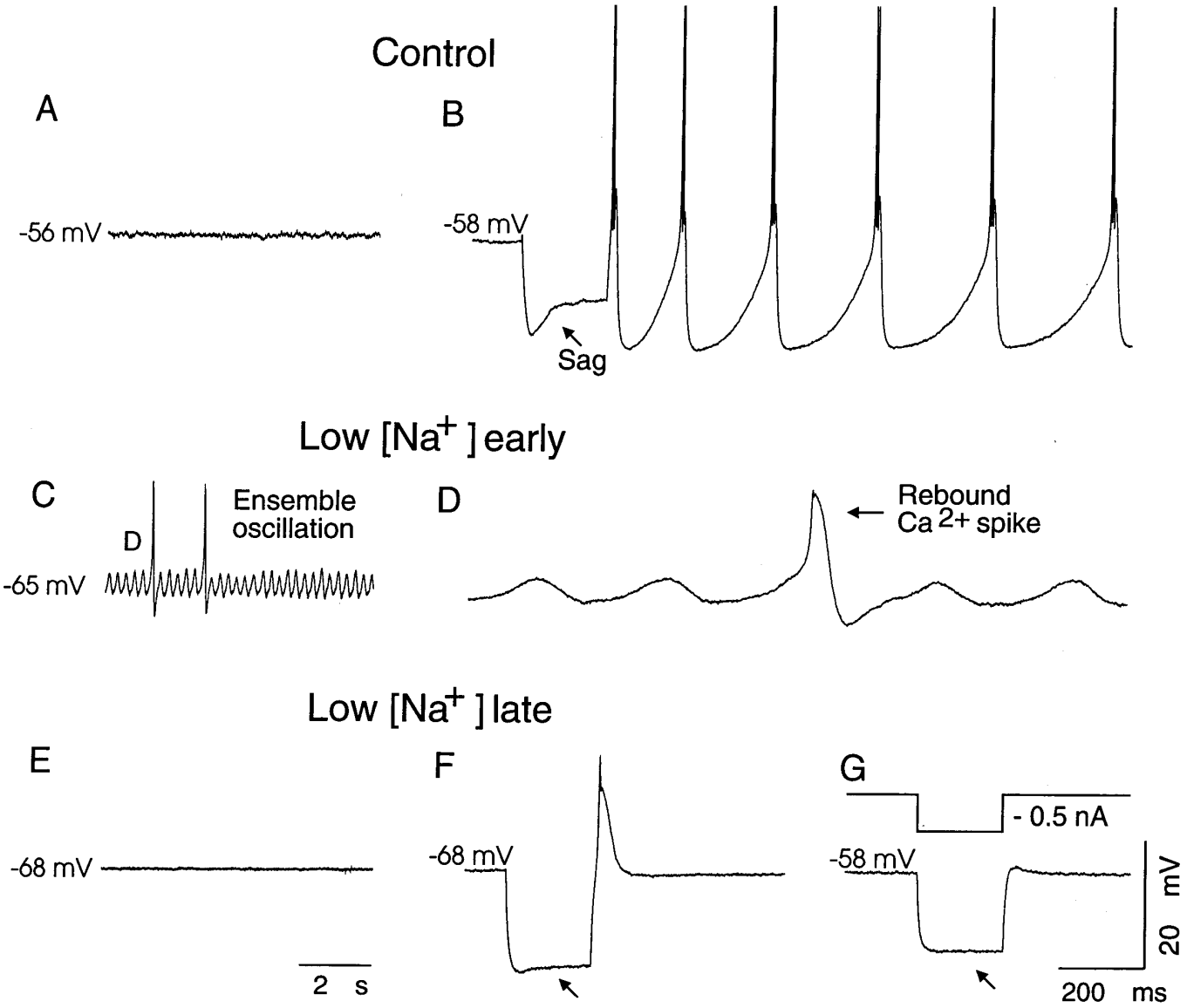

FIG. 8. Effects of reduction of extracellular concentration of Na^+ on IO cells. Before reduction of extracellular Na^+ concentration, no spontaneous rhythmic oscillations in membrane potential were seen (*A*) and intracellular injection of a hyperpolarizing current pulse was associated with a depolarizing sag and the generation of a rhythmic sequence of low-threshold Ca^{2+} spikes (*B;* spikes are truncated). Only a portion of the rhythmic oscillation is shown. Changing extracellular Na^+ concentration from 153.25 to 1.25 mM by substituting choline chloride for NaCl and choline bicarbonate for sodium bicarbonate in equimolar concentration in bathing medium resulted in steady hyperpolarization of neuron and appearance of rhythmic ''sine-wave'' oscillations in membrane potential (*C*) that could trigger generation of low-threshold Ca^{2+} spikes (*D*). After complete wash-in of low extracellular Na^+ concentration, rhythmic oscillations were blocked (*E*) and cell no longer generated fast action potentials nor oscillations on offset of current pulses, either at −68 or −58 mV (*F* and *G*). Data obtained from ferret IO. [Na^+], Na^+ concentration.

mic oscillations generated in response to a hyperpolarizing current pulse (Figs. 5*A* and 9*C*). Comparison of the rebound low-threshold Ca^{2+} spikes following the hyperpolarizing current pulse revealed a broadening of these with the application of either TTX or apamin accompanying the reduction of the AHP (Figs. 5*A* and 9*D*). This result suggests that the AHP considerably shortens the duration of the low-threshold Ca^{2+} spike.

DISCUSSION

The present results indicate that the activation of an inward current by hyperpolarization of the membrane contributes to the intrinsic and population oscillations of inferior olivary neurons. This current is sensitive to extracellular Cs^+ and is at least partly carried by Na^+ ions, and thus is likely to be I_h. The contribution of K^+ or Cl^- to I_h in inferior olivary neurons remains to be tested.

I_h generates the time-dependent rectification in IO neurons

The inward rectification first described in IO neurons by Yarom and Llinás (1987) shares common features with the effects generated by a class of hyperpolarization-activated current, termed I_h, described in a variety of electrically excitable

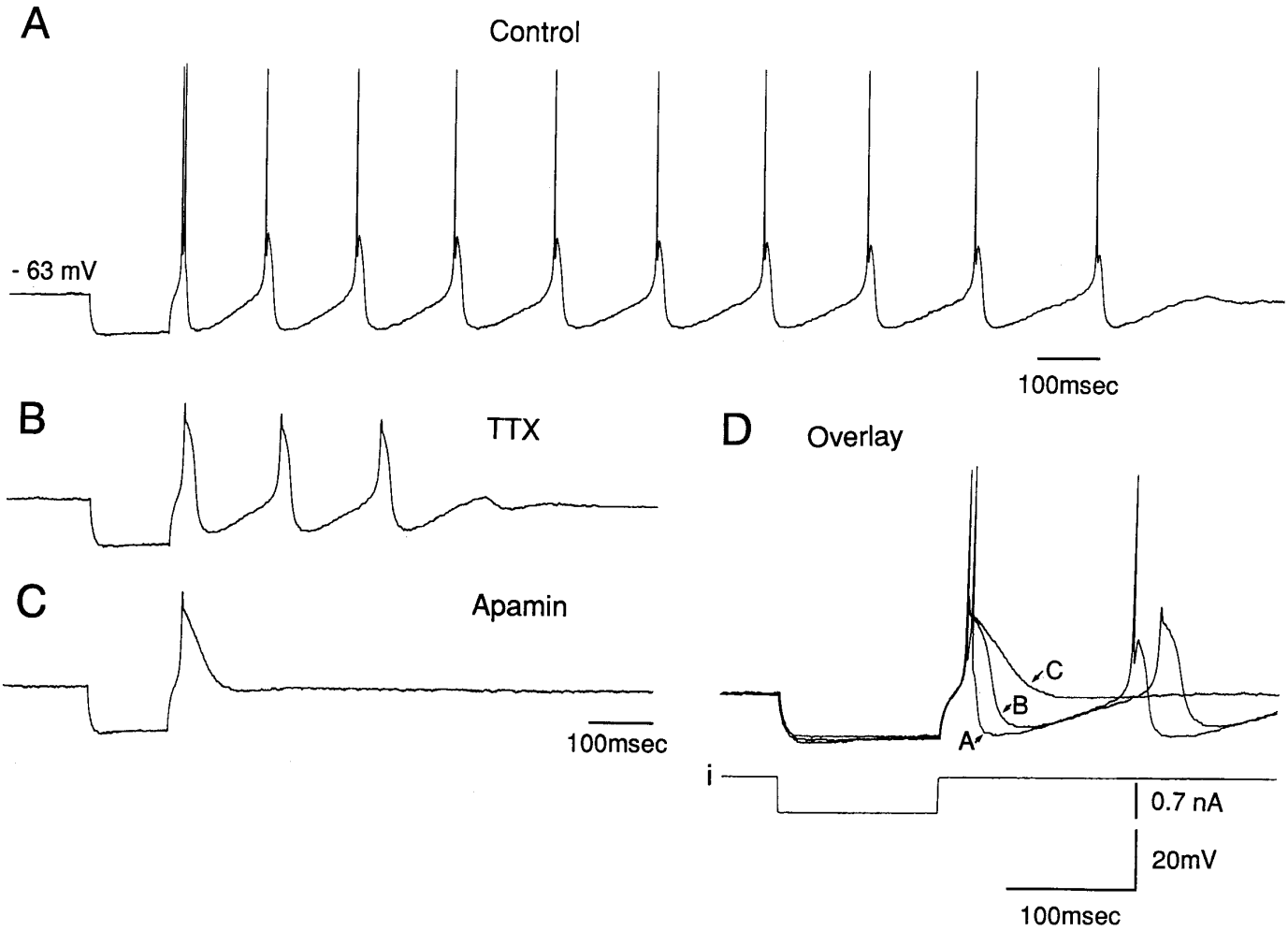

FIG. 9. Contribution of tetrodotoxin (TTX)- and apamin-sensitive currents to generation of rhythmic oscillations in IO neurons. *A*: intracellular injection of hyperpolarizing current pulse into IO neuron after block of depolarizing sag with extracellular application of Cs^+ is followed by a rhythmic sequence of low-threshold Ca^{2+} spikes interspersed with AHPs. *B*: block of voltage-dependent Na^+ currents with local application of TTX (10 μM in micropipette) results in a decrease in duration of oscillation. *C*: local application of apamin (100 nM in micropipette), a potent antagonist of some Ca^{2+}-activated K^+ currents, results in abolition of AHP and rhythmic oscillations. *D*: overlaying response to hyperpolarizing current pulse under these conditions reveals that although electrotonic response to current pulse did not change, block of voltage-dependent Na^+ currents with TTX resulted in a broadening of low-threshold Ca^{2+} spike and a small decrease in AHP (*B*). Application of apamin resulted in further broadening of low-threshold Ca^{2+} spike and complete abolition of AHP (*C*). Data obtained from guinea pig IO.

cells ranging from heart cells and axons (DiFrancesco and Noble 1989; Eng et al. 1990) to principal cells in the cerebral cortex, thalamus, and cerebellum (Crepel and Penit-Soria 1986; Halliwell and Adams 1982; McCormick and Pape 1990a; Spain et al. 1987). In all of these cell types, hyperpolarization of the membrane potential results in the slow activation of I_h, which is carried by both Na^+ and K^+ ions and therefore has a reversal potential of around −30 to −40 mV. At hyperpolarized membrane potentials, I_h is dominated by the entry of Na^+ ions into the cell, and therefore generates a slow depolarizing sag. The half-activation point in the steady-state activation curve for I_h varies between cell types, but is often in the range of −70 to −80 mV (McCormick and Pape 1990a). Because IO neurons are electrotonically coupled to one another, it is not possible to perform accurate voltage-clamp experiments on I_h in these cells. However, the block of the time-dependent inward rectification by extracellular application of Cs^+ (Figs. 3 and 4) or by replacement of extracellular Na^+ with choline$^+$ or $NMDG^+$ (Fig. 8) and the absence of block by extracellular Ba^{2+} (Yarom and Llinás 1987) indicate that the depolarizing sag generated in these neurons on hyperpolarization is due to the activation of I_h.

Contribution of I_h to the resting membrane potential

In other cell types, such as thalamic relay neurons, I_h not only generates a depolarizing sag on hyperpolarization, but also contributes to the determination of the resting membrane potential (e.g., McCormick and Pape 1990a). Similarly, I_h also appears to contribute strongly to the determination of the resting membrane potential and input conductance of IO neurons. In vitro, nonoscillating IO neurons have a resting membrane potential of −55 to −60 mV and are strongly hyperpolarized by the extracellular application of Cs^+ (Fig. 3) or reduction of the extracellular

concentration of Na^+ ions (Fig. 8). Interestingly, the partial reduction of I_h can hyperpolarize the cell into the range of membrane potentials at which the cell can intrinsically oscillate through the generation of rhythmic low-threshold Ca^{2+} spikes (Fig. 7). Persistent activation of I_h can therefore result in tonic depolarization of IO neurons, resulting in inactivation of the low-threshold Ca^{2+} current and a block of spontaneous rhythmic oscillations. Because IO neurons are electronically coupled to one another, the exact value of the resting membrane potential of each cell will depend on that of the other cells in the network.

The maintenance of the membrane potential of the cells in a ''silent'' region between rhythmic oscillations at hyperpolarized and depolarized membrane potentials may explain the general absence of spontaneous oscillatory activity in IO in vitro (Llinás and Yarom 1986; present results). However, even in the absence of spontaneous oscillations, the network of IO neurons displays a marked propensity to oscillate. For example, local electrical stimulation could induce prolonged (1–40 s) periods of 4- to 8-Hz synchronous oscillations in the IO (Fig. 1).

Contribution of I_h to oscillations in the inferior olive

The pioneering work of Llinás and Yarom (1981a,b) demonstrated that inferior olivary neurons can generate two distinct intrinsic oscillations that differ in frequency. A 3- to 6-Hz oscillation occurs at depolarized membrane potentials and is generated through the activation of a fast combined Na^+ and high-threshold Ca^{2+}-mediated action potential that activates a large and long-lasting AHP generated through a Ca^{2+}-activated K^+ conductance. The rising phase of the AHP was proposed to then activate a low-threshold Ca^{2+} spike, which reinitiated the cycle by activating again the Na^+/Ca^{2+} action potential. In hyperpolarized IO neurons, these cells generate a 9- to 12-Hz oscillation through similar mechanisms, although at a higher frequency owing to a decrease in the involvement of the dendritic high-threshold Ca^{2+} currents, resulting in a shortening of the duration of the AHP (Llinás and Yarom 1981a,b, 1986). Our data are consistent with this hypothesis for the generation of rhythmic oscillations in inferior olivary neurons, but also demonstrate an important role for I_h.

In our scenario, rhythmic oscillations at hyperpolarized membrane potentials in IO neurons are generated through the following sequence of events: activation of a somatic low-threshold Ca^{2+} spike, which generates one or two Na^+- and K^+-dependent action potentials, is followed by an AHP mediated largely by the activation of an apamin-sensitive

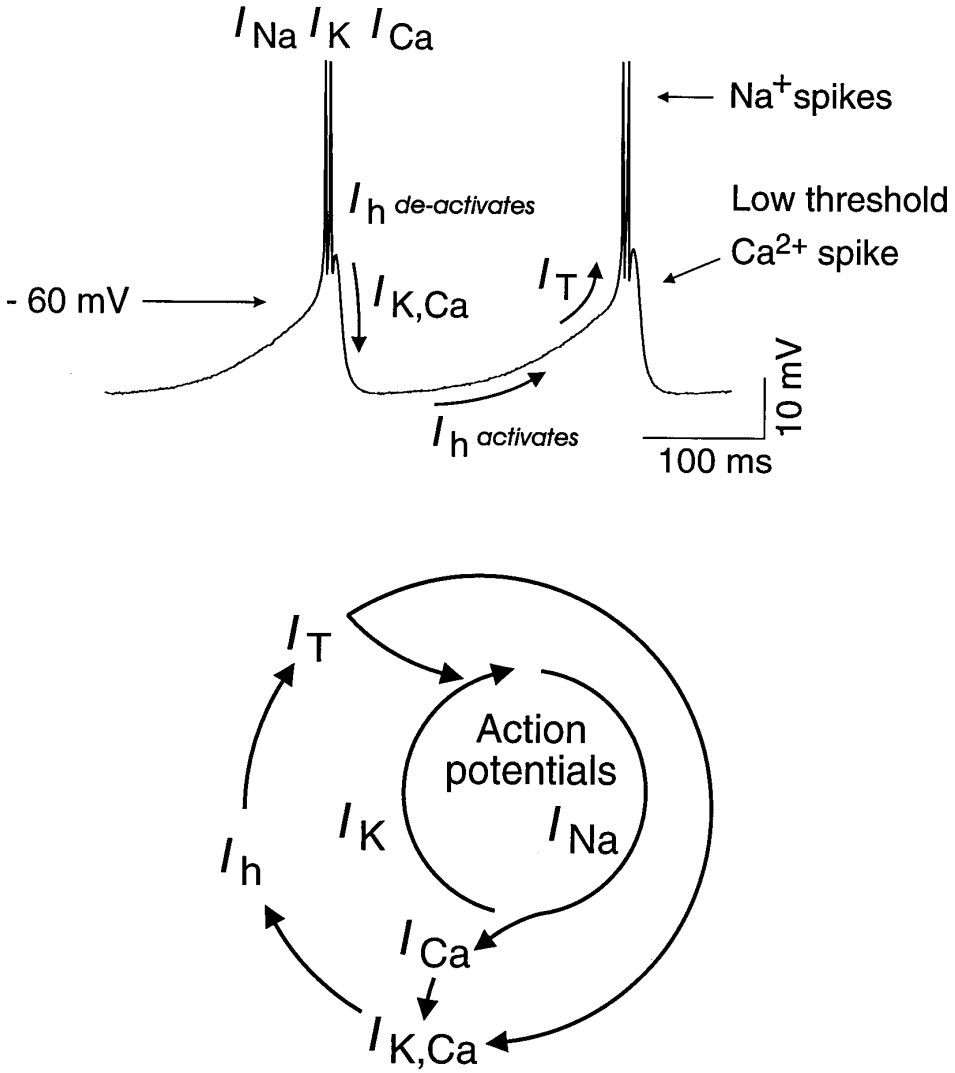

FIG. 10. Summary diagram indicating possible contribution of hyperpolarization-activated cation current I_h to rhythmic oscillations in IO. Rhythmic burst firing is created through generation of a low-threshold Ca^{2+} current (I_T), which activates fast action potentials mediated by Na^+, K^+, and Ca^{2+} currents (I_{Na}, I_K, and I_{Ca}, respectively). Entry of Ca^{2+} during generation of these fast action potentials and during generation of low-threshold Ca^{2+} spike results in generation of an AHP through activation of a Ca^{2+}-activated K^+ current. AHP activates I_h. Combined activation of I_h and decrease of a Ca^{2+}-activated K^+ current ($I_{K,Ca}$) results in depolarization of neuron, which activates another low-threshold Ca^{2+} spike. In this manner, I_h modulates frequency of oscillation. In addition, tonic activation of I_h also contributes to average membrane potential, and therefore to presence, strength, and frequency of oscillation in these neurons. Data obtained from guinea pig IO.

Ca^{2+}-activated K^+ current (Fig. 10). In addition, during the low-threshold Ca^{2+} spike and the generation of action potentials, a portion of I_h is deactivated. This deactivation of I_h facilitates the generation of the AHP by allowing it to reach more negative membrane potentials (Fig. 10). The AHP subsequently results in two important effects: removal of inactivation of I_T and the activation of I_h. Activation of I_h depolarizes the membrane potential toward the threshold for activation of I_T and subsequently promotes the generation of a low-threshold Ca^{2+} spike and associated Na^+- and K^+-dependent action potential(s), and therefore reinitiates the oscillation. In our recordings, rhythmic oscillations in IO neurons occurred at frequencies of between 6 and 10 Hz, but may occur at frequencies as low as 3 Hz after block of I_h.

The reduction of the rate of rise of the pacemaker potential between low-threshold Ca^{2+} spikes in IO neurons by application of extracellular Cs^+ gives experimental support to the hypothesis that I_h contributes to the generation of the pacemaker potential and the determination of oscillation frequency. Similar results have been obtained in pacemaker cells of the sinoatrial node of rabbit (Denyer and Brown 1990). The robust spontaneous pacemaking activity of the sinoatrial node cells was reduced in frequency by ~30% after block of the hyperpolarization-activated current I_f (which is homologous to I_h) by the extracellular application of 2 mM Cs^+. As in IO neurons, the reduction of I_f in sinoatrial cells was accompanied by a marked decrease in the slope of the pacemaker potential between action potential generation. Similarly, the activation of I_h also generates a pacemaker potential in single thalamocortical neurons and, through the interaction with the low-threshold Ca^{2+} current, can generate rhythmic burst firing in the frequency range of 0.5–4 Hz (McCormick and Pape 1990a). However, in these cells, complete block of I_h results in the suppression of rhythmic burst firing owing to the lack of a prominent AHP following low-threshold Ca^{2+} spikes in these cells in the absence of I_h.

Contribution of I_h to ensemble oscillation

Simultaneous hyperpolarization of inferior olivary neurons seems to be a condition under which synchronous sine-wave oscillation and rhythmic firing can be generated among IO cells. Application of the alkaloid harmaline on IO cells, in addition to blocking the time-dependent inward rectification (sag) (Yarom and Llinás 1987), also results in hyperpolarization of the cells and appearance of ensemble oscillation (Llinás and Yarom 1986). In the present study we demonstrate that bath application of low concentration of cesium or removal of extracellular Na^+ ions hyperpolarizes IO cells and results in generation of robust sine-wave oscillations that derive from the combined generation of rhythmic activity in the coupled network of IO neurons. These rhythmic oscillations of the membrane potential served to coordinate the rhythmic activity in the intracellularly recorded cell such that each low-threshold Ca^{2+} spike and subsequent action potentials were in synchrony with those of other neurons (Figs. 7 and 8). Therefore, by controlling the value of the membrane potential, I_h may play a key role in determining the generation and frequency of ensemble oscillations in the IO. Interestingly, in several different cell types including thalamic relay neurons (McCormick and Pape 1990b), brain stem cells (Bobker and Williams 1989), and heart neurons (DiFrancesco 1985), the voltage dependence of I_h is modulated by the activation of a variety of receptor subtypes. A similar type of modulation of I_h in IO cells could play an important role in the generation of normal (e.g., movement-related) and abnormal (e.g., tremor-related) network oscillations in the IO.

This work was supported by grants from the National Institutes of Health to D. A. McCormick, and from the Centre National de la Recherche Scientifique and the Fondation pour la Recherche Médicale to T. Bal.

Address for reprint requests: D. A. McCormick, Section of Neurobiology, Yale University School of Medicine, 333 Cedar St., New Haven, CT 06473.

Received 15 November 1996; accepted in final form 4 February 1997.

REFERENCES

AGHAJANIAN, G. K. AND RASMUSSEN, K. Intracellular studies in the facial nucleus illustrating a simple new method for obtaining viable motoneurons in adult rat brain slices. *Synapse* 3: 331–338, 1989.

ARMSTRONG, D. M., ECCLES, J. C., HARVEY, R. J., AND MATTHEWS, P.B.S. Responses in the dorsal accessory olive of the cat to stimulation of hind limb afferents. *J. Physiol. Lond.* 194: 125–145, 1968.

BELL, C. C. AND KAWASAKI, T. Relations among climbing fibre responses of nearby Purkinje cells. *J. Neurophysiol.* 35: 155–169, 1972.

BENARDO, L. S. AND FOSTER, R. E. Oscillatory behavior in inferior olive neurons: mechanism, modulation, cell aggregates. *Brain Res. Bull.* 17: 773–784, 1986.

BOBKER, D. H. AND WILLIAMS, J. T. Serotonin augments the cation current I_h in central neurons. *Neuron* 2: 1535–1540, 1989.

BOWER, J. AND LLINÁS, R. Simultaneous sampling of the responses of multiple, closely adjacent, Purkinje cells responding to climbing fiber activation. *Soc. Neurosci. Abstr.* 9: 607, 1983.

CREPEL, F. AND PENIT-SORIA, J. Inward rectification and low threshold calcium conductance in rat cerebellar Purkinje cells. An in vitro study. *J. Physiol. Lond.* 372: 1–23, 1986.

DE MONTIGNY, C. AND LAMARRE, Y. Rhythmic activity induced by harmaline in the olivo-cerebello-bulbar system of the cat. *Brain res.* 53: 81–95, 1973.

DENYER, J. C. AND BROWN, H. F. Pacemaking in rabbit isolated sino-atrial node cells during Cs^+ block of the hyperpolarization-activated current i_f. *J. Physiol. Lond.* 429: 401–409, 1990.

DIFRANCESCO, D. The cardiac hyperpolarizing-activated current, I_f, origins and developments. *Prog. Biophys. Mol. Biol.* 46: 163–183, 1985.

DIFRANCESCO, D. AND NOBLE, D. The current I_f and its contribution to cardiac pacemaking. In: *Neuronal and Cellular Oscillators*, edited by J. W. Jacklet. New York: Dekker, 1989, p. 31–57.

ECCLES, J. C., LLINÁS, R., AND SASAKI, K. The excitatory synaptic action of climbing fibres on the Purkinje cells of the cerebellum. *J. Physiol. Lond.* 182: 268–296, 1966.

ENG, D. L., GORDON, T. R., KOCSIS, J. D., AND WAXMAN, S. G. Current clamp analysis of a time-dependent rectification in rat optic nerve. *J. Physiol. Lond.* 421: 185–202, 1990.

FUKUDA, M., YAMAMOTO, T., AND LLINÁS, R. Simultaneous recordings from Purkinje cells of different folia in the rat cerebellum and their relation to movement. *Soc. Neurosci. Abstr.* 13: 603, 1987.

HALLIWELL, J. V. AND ADAMS, P. R. Voltage-clamp analysis of muscarinic excitation in hippocampal neurons. *Brain Res.* 250: 71–92, 1982.

JAHNSEN, H. AND LLINÁS, R. Electrophysiological properties of guinea-pig thalamic neurons: an in vitro study. *J. Physiol. Lond.* 349: 205–226, 1984a.

JAHNSEN, H. AND LLINÁS, R. Ionic basis for the electroresponsiveness and oscillatory properties of guinea-pig thalamic neurons in vitro. *J. Physiol. Lond.* 349: 227–247, 1984b.

LLINÁS, R. The intrinsic electrophysiological properties of mammalian neurons: insights into central nervous system function. *Science Wash. DC* 242: 1654–1664, 1988.

LLINÁS, R., BAKER, R., AND SOTELO, C. Electrotonic coupling between neurons in cat inferior olive. *J. Physiol. Lond.* 37: 560–571, 1974.

LLINÁS, R. AND SASAKI, K. The functional organization of the olivo-cerebel-

lar system as examined by multiple Purkinje cell recordings. *Eur. J. Neurosci.* 1: 587–602, 1989.

LLINÁS, R. AND VOLKIND, R. A. The olivocerebellar system: functional properties as revealed by harmaline-induced tremor. *Exp. Brain Res.* 18: 69–87, 1973.

LLINÁS, R. AND WELSH, J. P. On the cerebellum and motor learning. *Curr. Opin. Neurobiol.* 3: 958–965, 1993.

LLINÁS, R. AND YAROM, Y. Oscillatory properties of guinea-pig inferior olivary neurones and their pharmacological modulation: an in vitro study. *J. Physiol. Lond.* 376: 163–182, 1986.

LLINÁS, R. AND YAROM, Y. Electrophysiology of mammalian inferior olivary neurones in vitro. Different types of voltage-dependent ionic conductances. *J. Physiol. Lond.* 315: 549–567, 1981a.

LLINÁS, R. AND YAROM, Y. Properties and distribution of ionic conductances generating electroresponsiveness of mammalian inferior olivary neurones in vitro. *J. Physiol. Lond.* 315: 569–584, 1981b.

MAYER, M. L. AND WESTBROOK, G. L. A voltage-clamp analysis of inward (anomalous) rectification in mouse spinal sensory ganglion neurones. *J. Physiol. Lond.* 340: 19–45, 1983.

MCCORMICK, D. A. AND HUGUENARD, J. R. A model of the electrophysiological properties of thalamocortical relay neurons. *J. Neurophysiol.* 68: 1384–1400, 1992.

MCCORMICK, D. A. AND PAPE, H.-C. Properties of a hyperpolarization-activated cation current and its role in rhythmic oscillation in thalamic relay neurones. *J. Physiol. Lond.* 431: 291–318, 1990a.

MCCORMICK, D. A. AND PAPE, H.-C. Noradrenergic and serotonergic modulation of a hyperpolarization-activated cation current in thalamic relay neurones. *J. Physiol. Lond.* 431: 319–342, 1990b.

MCCORMICK, D. A. AND WILLIAMSON, A. Modulation of neuronal firing mode in cat and guinea pig LGNd by histamine: possible cellular mechanisms of histaminergic control of arousal. *J. Neurosci.* 11: 3188–3199, 1991.

SASAKI, K. AND LLINÁS, R. Dynamic electrotonic coupling in mammalian inferior olive as determined by simultaneous multiple Purkinje cell recording (Abstract). *Biophys. J.* 47: 53a, 1985.

SOLTESZ, I., LIGHTOWLER, S., LERESCHE, N., JASSIK-GERSCHENFELD, D., POLLARD, C. E., AND CRUNELLI, V. Two inward currents and the transformation of low frequency oscillations of rat and cat thalamocortical cells. *J. Physiol. Lond.* 441: 175–197, 1991.

SPAIN, W. J., SCHWINDT, P. C., AND CRILL, W. E. Anomalous rectification in neurons from cat sensorimotor cortex in vitro. *J. Neurophysiol.* 57: 1555–1576, 1987.

TABATA, T. AND ISHIDA, A. T. Transient and sustained depolarization of retinal ganglion cells by I_h. *J. Neurophysiol.* 75: 1932–1943, 1996.

VALLBO, A. B. AND WESSBERG, J. Organization of motor output in slow finger movements in man. *J. Physiol. Lond.* 469: 673–691, 1993.

WELSH, J. P., LANG, E. J., SUGIHARA, I., AND LLINÁS, R. Dynamic organization of motor control within the olivocerebellar system. *Nature Lond.* 374: 453–457, 1995.

YAMAMOTO, T., FUKUDA, M., AND LLINÁS, R. Bilateral synchronization of climbing fiber activity. *Soc. Neurosci. Abstr.* 12: 577, 1986.

YAROM, Y. AND LLINÁS, R. Long-term modifiability of anomalous and delayed rectification in guinea pig inferior olivary neurons. *J. Neurosci.* 7: 1166–1177, 1987.